Journal of Carcinogenesis
Covering Genesis to Therapeutics

Journal of Carcinogenesis, ISSN: 1477-3163
2025; Vol 24: Issue 9s, https://carcinogenesis.com/

Development, optimization and Characterization of novel Cetuximab conjugated, Lycopene encapsulated PLGA-Alginate nanoparticles for an enhanced cytotoxicity of Lycopene in PANC-1 cells

Mohini Singh[*1], Venessa Nath[1], Rajat Subhra Dutta[2], Anup Kumar Das [3], Bani Kumar Jana1, Ananya Rajkumari[1], Sorra Sandhya[1], Bhaskar Mazumder[1]

[1]Department of Pharmaceutical sciences, Dibrugarh University, Dibrugarh,Assam, 786004.

[2]Girija Nanda Choudhry Institute of Pharmaceutical Sciences, Tezpur Assam India,784501,

[3]Department of Pharmaceutical Science, Assam Central University, Silchar, Assam, India, 788011.

ABSTRACT

This study aims to mitigate pancreatic cancer by developing Cetuximab-conjugated Sodium Alginate- Poly (lactic-co-glycolic acid) (PLGA) nanoparticles loaded with Lycopene. Although Lycopene, a strong antioxidant found in tomatoes, has shown strong anti-cancer effects, its poor solubility and stability limit its therapeutic use. Lycopene is encapsulated in nanoparticles made of a hybrid combination of Sodium Alginate and PLGA matrix which Alginate increases the encapsulation efficacy of Lycopene, increases its solubility and guarantees a regulated release. To attain the required particle size, zeta potential, and drug encapsulation effectiveness, a number of factors were methodically adjusted by using Design of expert software and following the Box Behenken design, including the formulation's stirring speed (rpm) and the content of Sodium Alginate and surfactant (Tween 80). The formulationshowed a negative zeta potential, a good drug loading and encapsulation capacity, and an average particle size of roughly 154 nm. The optimised nanoparticles was conjugated with Cetuximab and the amount conjugated monoclonal antibody was estimated using Bradford's protein assay. Moreover, the haemolytic toxicity study indicated a compatible nature of the formulation with RBC's with no evident hemolysis. Finally, the optimized formulation showed and enhanced cytotoxicity in PANC-1 cell linens in comparison to pure Lycopene. We attribute this to the fact that the optimized formulation showed an enhanced cellular uptake and better cellular internalization, making it a very promising drug delivery tool for Pancreatic ductal adenocarcinoma.

KEYWORDS: *Pancreatic cancer and the role of Lycopene, Lycopene and its bioavailability*

How to Cite: Mohini Singh, Venessa Nath, Rajat Subhra Dutta, Anup Kumar Das, Bani Kumar Jana, Ananya Rajkumari, Sorra Sandhya, Bhaskar Mazumder., (2025) Development, optimization and Characterization of novel Cetuximab conjugated, Lycopene encapsulated PLGA-Alginate nanoparticles for an enhanced cytotoxicity of Lycopene in PANC-1 cells, *Journal of Carcinogenesis*, *Vol.24*, *No.9s*, 374-392.

1. INTRODUCTION

Pancreatic cancer and the role of Lycopene:

Pancreatic cancer is the fifth and fourth most common cause of cancer-related fatalities for men and women, respectively, according to global statistics for industrialised nations. Similar mortality rates for PanCA are also observed in other developed nations (1,2,3,4,5) Standard treatment regimen for pancreatic cancer (FOLFIRINOX and Gemcitabine) including neo-adjuvant techniques for treating pancreatic cancer have become popular recently. But, there is no quantum leap in survival rate of patients as there are plenty of drawbacks associated with these regimens like tumor resistance due to complex tumor environment and high off target toxicity leading to plenty of side effects (5,6,7,8). Hence there is an ongoing need to introduce new molecules that can fight pancreatic cancer and plant based caretenoids like Lycopene can play a very significant role as a lot of research work done in the past decade has proved that Lycopene has a significant anti cancer activity against a vast array of cancers, including Pancreatic cancer. It has also shown to inhibit vital molecular pathways like the NF-κB (nuclear factor kappa-light-chain-enhancer of activated B cells) pathway which plays a central role in signaling cascade reactions involved in regulating inflammation, immune response and cell survival in Pancreatic cancer. The only issue that stands in the way of efficient drug delivery of Lycopene to the tumor cells is its poor water solubility. (3,4,5,10).

Lycopene and its bioavailability:
Lycopene is an organic compound with a molecular weight of 536.85 g·mol^{-1} and the chemical formula $C_{40}H_{56}$. While it is soluble in certain organic solvents, it is insoluble in water. Eleven of the thirteen double bonds in its molecular backbone are conjugated, giving Lycopene its potent red colour and antioxidant nature. Recent developments in nanotechnology could offer practical solutions to Lycopene's disadvantages. The bulk of studies on nano-carotenoids have focused on creating nano-sized carriers for the pigments via nanotechnology, evaluating and characterizing their stability, and investigating their release, bioavailability, and pharmacological activity in vitro (11,12). Simultaneously, the field of nano-scale bioactive delivery vehicles has experienced rapid development. The most common examples of these carriers in this scenario are metallic nanoparticles, biopolymeric nano-structures and lipid-based nanoformulations. Nazemiyeh et al in their study did formulation followed by physico-chemical characterization of some Lycopene- Solid Lipid Nanoparticles In summary, this study produced stable Lycopene-SLNs with good physicochemical properties that are a good fit for upcoming in vivo trials in the nutraceutical industry (13,14,15,16,18). In on of the 2022-based studies, Goswami A et al. prepared Lycopene-loaded polymeric nanoparticles for the treatment of prostate cancer and optimized the formulation by Box-Behnken design followed by cytotoxicity investigations [19]. Carvallo GC et al prepared mesoporous silica nanoparticles (MSNs) that were used in this work to load and shield LYC from deterioration, followed by evaluating its efficacy in vulvovaginal candidiasis (20). Mennati A et al in a 2022 based research, achieved double-silencing of the insulin-like growth factor 1 receptor in MCF-7 breast cancer cell line by simultaneous delivery of of siRNA and Lycopene-encapsulated hybrid lipid nanoparticles (21,22). In a 2023 based study, Guo S, et al. prepared enzymatically cross-linked Lycopene encapsulated α-lactalbumin nanoparticles greatly increased photostability and loading capacity for the Lycopene.

EGFR Medaited active targetting in PANC- 1 cells.
The tyrosine kinase family includes the transmembrane glycoprotein known as the epidermal growth factor receptor. EGFR is a key player in initiating two major signalling pathways in a typical cell. Apoptosis, angiogenesis, and chemotherapy/radiotherapy resistance are among the several cancer-related signalling pathways that EGFR is linked to.14. In 30–89% of cases of pancreatic ductal carcinoma, EGFR is overexpressed.Since nanoparticles have been employed to try to increase the effectiveness of anticancer treatment, employing EGFR's ligand, EGFR, for nanoconjugation has shown encouraging results in boosting the targeted cells' cellular uptake processes and death [23,24,25].

2. MATERIALS AND METHODS:

2.1 Materials:
Lycopene was a gift sample from Alpha Remedies, Ambala, India. Poly (lactic-co-glycolic acid) (PLGA) 85:25 and Cetuximab were purchased from Sigma Aldrich, St. Louis, MO, USA., Sodium Alginate, Calcium Chloride, Tween 80, Dichloromethane (DCM), Octanol, Sodium Chloride, Potassium di-hydrogen Phosphate, Di-sodium hydrogen phosphate, Hydrochloric acid, N-hydroxysuccinimide(NHS,),1-Ethyl-3-(3-diaminopropyl) carbodiimide (EDC), Hexane and Mannitol were purchased from Hi-Media Laboratories, Pvt. Ltd., LBS Marg, Mumbai, India

2.2 Methods:
2.2.1 Pre-Formulation Study:
Preformulation studies are a vital component in the pharmaceutical development process, providing essential information that lays the groundwork for the formulation of safe, effective, and stable drug products. Preformulation study's main goal is to provide data and information on a drug substance and manufacturing technology before formulation development activities and product design for a drug product are initiated (26). These studies encompass a series of comprehensive investigations into the physicochemical properties of a drug substance before formulation, aimed at understanding its behaviour, characteristics, and compatibility with various excipients and manufacturing processes. Compatibility studies are crucial to ensure that the drug substance remains stable when combined with excipients used in formulation. Overall, Preformulation studies serve as the cornerstone for subsequent formulation development, providing crucial insights into drug behaviour and aiding in the design of safe, effective, and stable pharmaceutical products (26, 27,28).

2.2.1.1 Determination Of (Λ_{max}) Using UV- VIS Spectroscopy and preparation of calibration curve:
Determination of wavelength of maximum absorbance (λ_{max}) of Lycopene in different mediums followed by preparation of standard curves for further crucial investigations involved in characterization step of nanoparticles. The (λ_{max}) of drugs in different mediums (such as phosphate buffer 7.4, phosphate buffer 6.8 and organic solvent dichloromethane) were scanned using a UV Visible spectrophotometer. The stock solution (1000 ppm) of Lycopene was prepared in each medium separately. Then the stock solution was diluted and were scanned in UV- Vis Spectrophotometer under spectrum mode in the wavelength range of 200-800 nm and the peak table in all solutions was recorded.(29)

For standard curve, the stock solution (1000ppm) of the drug was prepared in each medium and was diluted serially using

the same dissolution medium to make a sample of concentration of 10, 20, 30, 40, 50, 60 and 70 ppm. The absorbance of all these samples was measured using UV-Vis spectroscopy at obtained (λmax).

2.2.1.2 Drug-Excipients Compatibility Study using FT-IR Spectroscopy:
Drug sample (Lycopene), excipients (PLGA, Sodium alginate, Calcium Chloride, Tween 80) and physical mixture in 1:1 ratio were characterized by FTIR spectroscopy. FT-IR analysis is used to identify the drug samples. It measures a sample's absorbance of infrared radiation at various wavelength to determine the sample's molecular composition and structure. The spectrum was recorded using FT-IR spectrophotometer (Alpha, Bruker, Germany) over a range of 4000-500 cm^{-1}. The spectrum of the drug was compared to the standard spectra to confirm the identity of the drug. The recorded spectrum was recorded and interpretated (30,31).

2.2.1.3 Differential Scanning Calorimetry (DSC)
Differential scanning calorimetry (DSC) is a thermo-analytical technique, used for thermal analysis of lycopene. Samples were analysed using Jade DSC (Perkin Elmer, Japan). The required amount of drug sample was placed in an aluminium pan that is completely sealed and heated at 10^0C/ min, with nitrogen purging at 20ml/min over a temperature ranging from 30^0 C to 450^0 C (32).

2.2.2 Preparation of Lycopene-encapsulated Alginate-PLGA Nanoparticles, using Single Emulsion Solvent-Evaporation Method:
Lycopene-loaded Alginate-PLGA nanoparticles were prepared using single emulsion solvent evaporation method. About 10mg of lycopene was taken and dissolved in 2.5 ml of dichloromethane (DCM). To this 20mg of polymer PLGA poly (lactic-co-glycolic acid) (85:15) was added to form the organic phase. Drug: Polymer ratio= 1:2. To the aqueous phase 1% of sodium alginate (A biopolymer to form a coating around the nanoparticles, providing additional stability and controlled release properties) was added along with Tween 80(surfactant) and stirred for 30 mins at 2000- 6000rpm. The resultant drug polymer solution was then added dropwise to the aqueous phase forming oil-in-water solution under vigorous stirring. The emulsion was stirred for 1-2 hrs continuously to evaporate DCM leading to the formation of PLGA nanoparticles encapsulating lycopene. A solution of 0.2% (w/v) calcium chloride ($CaCl_2$) was prepared that was dropwise added to the Alginate-coated nanoparticles under gentle stirring to crosslink the alginate, forming a stable coating around the nanoparticles. The consequential solution was then sonicated for 45 minutes followed by gentle magnetic stirring for 1-2 hours to eliminate the organic solvent completely. Then the solution was centrifuged twice. Firstly, at 5000 rpm for 5 minutes from where the supernatant residue was collected and then againsubjected to centrifugation at 15000 rpm for 30 minutes. The supernatant was collected and then finally freeze dried to get the nanoparticles (33,34,35).

2.2.3 Formulation optimazation using Design of Experiment (DoE):
The thorough literature review gives numerous data on various parameters so as to optimize the formulations. In this study, the 3-level factorial Box-Behnken design (BBD) of Design Expert (version 10.0.3) software isused for the above mentioned purpose of optimization. The optimization process involves setting up a Box-Behnken design matrix where the independent variables (stirring speed, sodium alginate concentration, and Tween 80 concentration) are varied systematically across three levels. This results in a set of experimental runs where each factor is tested at high and low values. The responses (particle size, zeta potential, and drug entrapment efficiency) are measured for a set of 17runs. A second-order polynomial equation is then fitted to the experimental data to model the relationship between the independent and dependent variables. Analysis of variance (ANOVA) is performed to determine the statistical significance of the model and the interaction effects. The optimization seeks to identify the combination of factor levels that minimize particle size, maximize zeta potential (for better stability), and maximize drug entrapment efficiency. The desirability function approach is often used to combine these multiple responses into a single composite desirability score, guiding the selection of the optimal formulation conditions (36,37,38).

2.2.4 Characterization of Lycopene -Loaded PLGA Nanoparticles
2.2.4.1 Percentage yield of the PLGA nanoparticles

After formulating the nanoparticles, the Yield (%) was calculated by the following formula (39):

$$Yeild\ (\%) = \frac{Weight\ of\ Nanoparticles}{Weight\ of\ drug\ and\ polymer\ used\ for\ nanoparticle\ preparation} x100$$

2.2.4.2 Drug Loading and Entrapment Efficiency Determination
For the determination of drug loading and entrapment efficiency, an accurately weighed amount of 2mg of Lycopene loaded nanoparticles were to be placed into a centrifuge tube, and 2 mL of DCM is to be added to it. Then it will be continuously shaken for 3–4 hours at 37°C in an incubator shaker. The dispersed phase will detach from the continuous phase by

centrifugation. Then the supernatant is to be acquired and thedrug that is present is to be assayed spectrophotometrically. The percentage drug loading and entrapment efficiency is to be calculated by means of the applicatiion of the equation stated as follows- (4)

$$\%Drug\ Entrapment\ efficacy = \frac{Amountof\ drug\ present\ in\ nanoparticles}{Initial\ amount\ of\ drug\ added}\ x100$$

2.2.4.3 Estimation of Particle Size and Particle size Distribution Analysis:
Litesizer Anton Paar was used for particle size and distribution characterization. The instrument is equipped with a solid-state laser, which employ dynamic light scattering (DLS). Appropriate amount of the dried nanoparticles formulation is to be suspended in distilled water and sonicated for an appropriate period prior to the measurement. The resulted homogeneous suspension will then determine for the average hydrodynamic particle size, size distribution and polydispersity index (40).

2.2.4.4 Zeta Potential Measurement (ZP):
Zeta potential measurements is to be done by using Litesizer Anton Paar. Suitable amount of the dried nanoparticles from each formulation were suspended in distilled water and are to be sonicated for an appropriate period prior to the measurement; the ZP characterizes the particle surface charge and gives information about long term stability (40).

2.2.5 Conjugation of Cetuximab to Optimized Alginate-PLGA Nanoparticles.
The Cetuximab antibody was tagged onto the nanoparticles surface by implementing N-hydroxysuccinimide (NHS) and 1-(3-dimethylaminopropyl)-3-ethylcarbodiimide hydrochloride (EDC) coupling chemistry. In brief, the carboxyl group of Lycopene-loaded PLGA nanoparticles will be activated by using EDC and NHS. Subsequently, a weighed quantity (5-10mg) of lyophilized nanoparticles was suspended in PBS (1 mg/1 mL). The prepared solution received 1 µL of antibody (from the primary stock). The resulting solution was then centrifuged at 8000 rpm for a time perioud of around 25 minutes to eliminate any residual antibodies before being incubated at 25°C for 1 h. Thereafter, the finished product was lyophilized and kept at 4°C (40,41) .

2.2.6 Characterization of Cetuximab conjugated PLGA nanoparticles by 1H-NMR
Characterizing Cetuximab-conjugated PLGA nanoparticles by Nuclear Magnetic Resonance (NMR) spectroscopy provide information on the molecular structure, confirmation of conjugation, and the interaction between Cetuximab and the nanoparticles. Solvent used was Dimethyl Sulfoxide (DMSO) and 1H NMR technique was employed to obtain information on the overall chemical environment and confirm the presence of PLGA and Cetuximab. The data was then interpreted that identifies the signals corresponding to the amino acids in Cetuximab along with some chemical shifts, peak splitting, or the appearance of new peaks that indicate the formation of covalent bonds between PLGA and Cetuximab (41).

2.2.7 Characterization of Cetuximab conjugated PLGA nanoparticles by FT-IR
Confirmation of conjugation of cetuximab to PLGA was analysed by Fourier transform infrared (FTIR) spectroscope in the transmission range of 4000 $cm^{-1}$to 400 cm^{-1}. Samples of Alginate-PLGA nanoparticles and Cetuximab conjugated Alginate-PLGA nanoparticles were formulated and lyophilized to form powder. The lyophilized samples were then analysed in FT-IR corresponding to a range of 4000 $cm^{-1}$to 400 cm^{-1}. The FTIR spectrum of both samples,were analysed to identify and interpret the corresponding characteristic peaks, evidence of the chemical bonding and conjugation efficiency that confirmed the conjugation of cetuximab to PLGA nanoparticles (41).

2.2.8 In-Vitro Release Study
2.2.8.1 In -vitro drug release of the optimized Lycopene- loaded Alginate-PLGA nanoparticles
Of the various methods used to assess drug release from nano-sized dosage forms, the dialysis method (DM) is the most versatile and popular. The in-vitro drug release analysis of Lycopene-encapsulated Alginate- PLGA nanoparticles formulation was done by dialysis bag diffusion method. The prepared nanoparticles(5 ml) were dispersed into a pre-soaked dialysis membrane which was then accurately sealed from both the ends. This formultion containg dialysis bag was suspended inside a beaker containing 90 ml of phpsphate buffer with a pH 7.4 and 6.8 respectively, assuring that its fully submerged. The beakes setup was then mounted on a magnetic stirrer and the set up temprature was maintained at 37 ± 2 °C throughout the duration of the experimentat an rpm of 100. The samples (5 ml) were withdrawn at fixed time intervals of 0, 1, 2, 4, 6, 8 and 24hrs and were substituted with respective fresh buffers. After suitable dilutions, the samples were analysed at UV-Visible spectrophotometer at a wavelength of 373 nm approximately (9).

2.2.8.2 Drug Release kinetic study of the formulation
The specific in vitro release data were analysed to identify the best fit model in several kinetic equations for better understanding of the process and kinetics of the drug release. The kinetic models of zero order, first order, Higuchi model,

Korsmeyer- Peppas's model and Hixon- Crowell's model were used to evaluate the release profile. The obtained value will indicate the best release mechanism for the prepared formulations (43).

2.2.9 High- Resolution Transmission Electron Microscopy (HR-TEM)

High-Resolution Transmission Electron Microscopy (HRTEM) is a powerful technique for characterizing Cetuximab-conjugated PLGA nanoparticles. HRTEM provides detailed images at the atomic or molecular scale, allowing for the visualization of the nanoparticles' size, shape, and surface morphology with high precision. When optimized Cetuximab-conjugated PLGA nanoparticles were analysed using HRTEM (JEM-2100 PLUS (HR), Jeol), it confirms the uniformity and structural integrity of theformulated nanoparticles. It enables the observation of the nanoparticle surface and morphology to verify the conjugation and distribution of Cetuximab on the PLGA matrix. The sample was diluted with ultra-pure water to prevent aggregation and ensure even distribution on the carbon coated TEM grid. A small amount of the sample was placed on the grid and allowed to dry and then negatively stained with 2% aqueous uranyl acetate solution. The sample was then analysed (44).

2.2.10 Haemolysis Study:

Haemolysis is the medical term used to describe the destruction of red blood cells. The haemolysis process is characterized by accelerated breakdown of the erythrocyte (RBC) membranes, releasing intra-erythrocyte content to the extracellular compartment. The freshly drawn blood from male Wistar rats was collected in anticoagulant-treated EDTA tubes. The blood sample was centrifuged at 1500 rpm for 10 minutes to separate the plasma and obtain the RBC pellet. The RBCs were washed with Phosphate Buffer by resuspending the pellet in PBS and centrifuging at 1500 rpm for 5 minutes. The RBCs were resuspended in PBS to obtain a 2% v/v RBC suspension. About 0.5ml of RBC suspension was then placed in 1ml microcentrifuge tubes and marked as (45,46)

a) Positive Control (Tap Water)
b) Negative Control (0.9% NaCl)
c) Blank PLGA (Blank PLGA formulation diluted with PBS)
d) Cet-PLGA (Cetuximab-conjugated PLGA nanoparticles dissolved in PBS)

Each tube was incubated at 37°C for 1 hour and then centrifuged at 4 °C for 5 min at 2500 rpm. For measurement of Haemolysis The absorbance of the supernatants was measured at 540 nm using a spectrophotometer. This wavelength corresponds to the absorbance of haemoglobin released from lysed RBCs (45,46).

2.2.10.1 Calculation of Haemolysis Percentage:

The observed haemolysis was calculated using the formula as follows:

$$Percentage\ Haemolysis = \frac{Abs.of\ sample - Abs\ of\ negative\ control}{Abs.of\ positive\ control - Abs.of\ negative\ control}$$

2.2.11 Bradford Protein Assay

The Bradford Protein Assay is a rapid and simple method for quantifying proteins, and it is used to measure the protein content of Cetuximab conjugated PLGA nanoparticles. To perform the Bradford Protein Assay for cetuximab-conjugated PLGA nanoparticles, a series of Bovin Serum Albumin (BSA) standards (50, 100, 150, 200, 250, 300 µg/mL) were prepared in PBS 7.4 to generate a standard curve. 10-20 µL of each BSA standard and nanoparticle samples (blank PLGA and cetuximab-conjugated PLGA) were dispensed into separate wells of a 96-well microplate. Around 200 µL of Bradford reagent was added to each of the well and incubated at 37^0C for 5-10 minutes. The absorbance was measured at 595 nm using a microplate reader. The standard curve of BSA concentration versus absorbance was plotted and then the protein concentration of the cetuximab in the nanoparticle samples was determined using the standard curve (47).

MTT-Assay on PANC-1 cell lines:

PANC-1 cell culture:

PANC-1 cell line was Procured from NCCS Pune. The cells were harvested from flask at 90% confluency and seeded in 96 well plates at appropriate density in DMEM medium (Dulbecco's Modified Eagle Medium-AT149-1L) supplemented with 10% FBS (Fetal Bovine Serum - HIMEDIA-RM 10432) and 1% antibiotic solution at 37°C with 5% CO_2. Next day, remove the medium and add fresh culture medium to each of the well of the plate and then added 5- 50 µl (10% of total medium of cell culture) of prepared treatment dilutions to the defined wells and it was incubated (Air-Jacketed CO_2 Incubator- Heal Force -HF90) for 24 hr. The cell culture becomes ready for further experimental studies [48].

2.7.9.11.2 MTT Assay on PANC-1 cells:

MTT assay was conducted to compare the cytotoxic potential of Lycopene (LY), Lycopene loaded Alginate-PLGA nanoparticles (LY-PLGA) and Lycopene loaded-Cetuximab conjugated PLGA nanoparticles (LY-PLGA-CET). Cells were

seeded at $1x10^4$ cells/well density in a 96 well tissue culture plate and incubated for 24 hours. After the treatment period, MTT was incorporated in the plate and incubated for an additional 3h in the CO_2 incubator. Thereafter, the medium was aspirated from every well and solubilisation media (DMSO) was added into the wells. The absorbance was taken at 570 nm using a multimode microplate reader and images were captured under inverted microscope (Olympus ek2) using Camera (AmScope digital camera 10 MP Aptima CMOS) [48,49].

3. REULTS AND DISCUSSIONS

6.1.5 UV- Vis Spectrum of Lycopene for determination of wavelength of maximum absorbance (λ_{max}) of Lycopene in different mediums and plotting of standard curve:

The (λ_{max}) of the drug was scanned in different mediums such as Dichloromethane (DCM), phosphate buffer pH 7.8 and 6.8, using UV-Visible spectrophotometer. The stock solution (1000 ppm) of Lycopene was prepared in each medium separately. Then the stock solution was diluted and scanned in UV-Visible Spectrophotometer under spectrum mode in the wavelength range of 200-600 nm and the λ_{max} of the drug in all the solutions was recorded and reported in Table No 1. This was followed by plotting the standard curves of Lycopene in the respective solvents as depicted in Figure No 1.The calibration curve in different solvents was plotted in corelation with Beer's Law, with concentration range from 5 to 25 ppm in the various solvents specified above to obtain the regression equation.

Table No.1 (λ_{max}) of Lycopene in various solvents.

Solvents	**Lycopene λ_{max}**
Dichloromethane (DCM)	478.0 nm
Phosphate buffer 7.4	373.50 nm
Phosphate buffer 6.8	371.50 nm

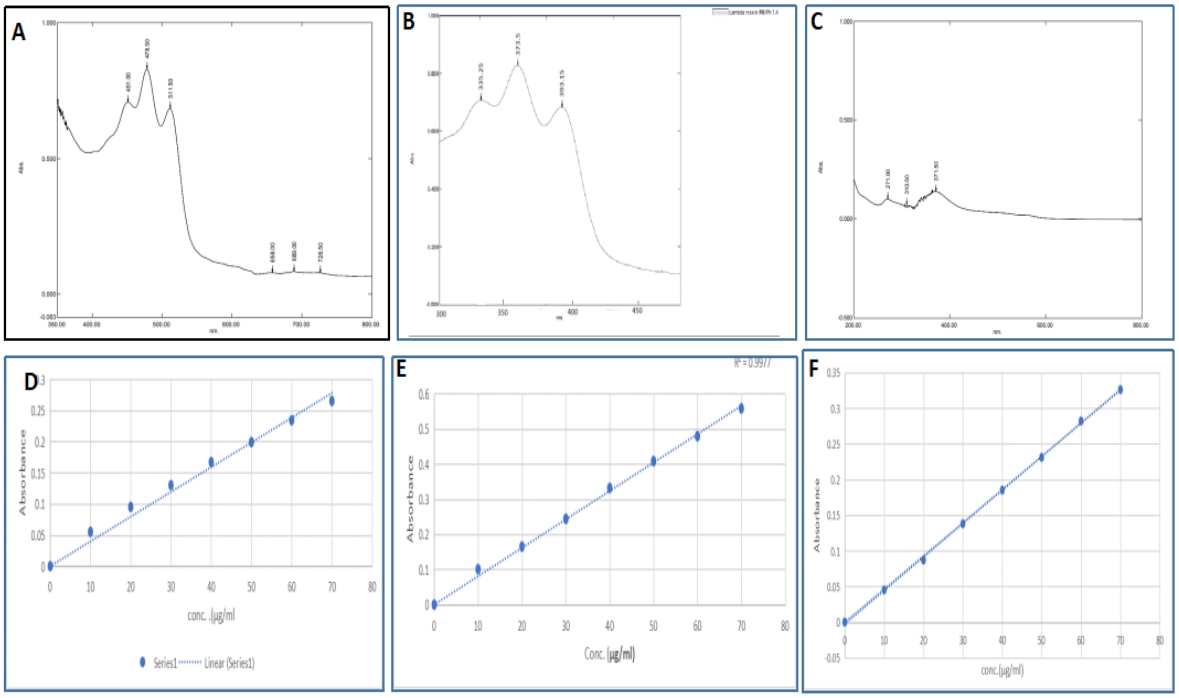

Figure No 1: A,B & C Respresent the lamda max of Lycopene in in Dichloromethane, Phosphate buffer pH 7.4 and 6.8. D ,E and F represent the the calibration curve of Lycopene in Dichloromethane, Phosphate buffer pH 7.4 and 6.8 respectively.

Drug-Excipients Compatibility Study Using FT-IR Spectroscopy:

FT-IR of pure drug lycopene, all the excipients (PLGA, sodium alginate, calcium chloride and tween 80) and physical mixture was recorded using FT-IR spectrophotometer (Alpha Bruker, Germany) within a range of 500- 4000 cm^{-1}. These spectrums were interpreted and were compared with the standard IR spectrumof Lycopene. . The spectrum of lycopene contains all the peaks of authentic sample. The FTIR spectrum of the physical mixture was quite similar to that of standard Lycopene all the major peaks were present as depicted in Figure No 2. The bands 2924.53 cm^{-1}, 2921.76 cm^{-1}, 2862.00 cm^{-}

[1], 2911.96 cm^{-1} and 2986.97 cm^{-1} were assigned to C-H stretch, 1735.03 cm^{-1}, 1734.62 cm^{-1}, 1739.97 cm^{-1}, were assigned to C=O stretch, 3681.09 cm^{-1}, 3484.20 cm^{-1}, 3376.16 cm^{-1} to O-H stretch respectively. This finding confirms that no change in observed in basic chemical backbone (46,47,50).

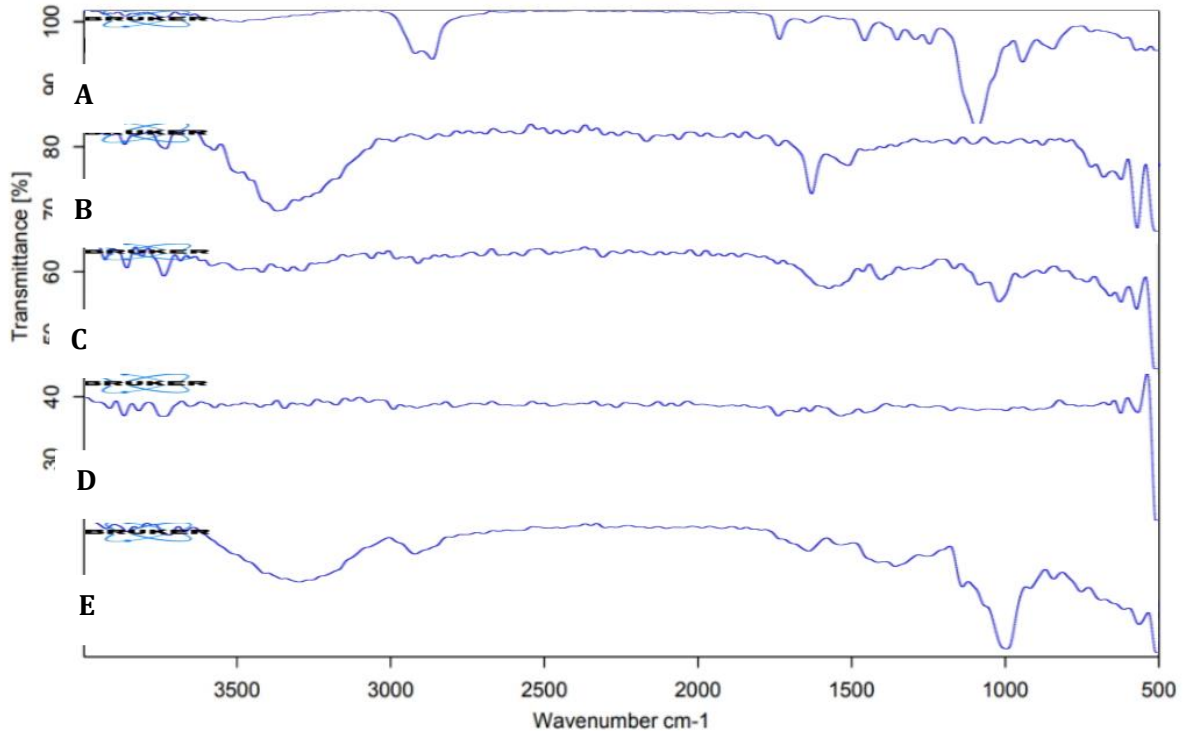

Figure 2: FT-IR of pure drug Lycopene (A), all the excipients, PLGA (B), Calcium Chloride (C) and Tween 80 (D) and physical mixture (E) was recorded using FT-IR spectrophotometer. The FTIR spectrum of the physical mixture was quite similar to that of standard Lycopene as all the major peaks were present indicating a compatibility between drug and excipient.

Differential Scanning Calorimetry (DSC)

DSC thermograph of the API (lycopene), polymer (PLGA) and physical mixture was recorded and shown in figure no.6.15, 6.16 and 6.17 respectively. The DSC thermogram of pure drug Lycopene was recorded that showed a sharp endothermic peak at 175.68^{0}C, corresponding to the melting point of Lycopene. The melting enthalpy (Delta H) was observed at 18.868 J/g and the area of peak was 188.687 mJ, with a peak height of 6.9256 mW (5). The DSC thermogram of polymer PLGA was recorded that showed a very sharp endothermic peak specifically at 295.28^{0}C, corresponding to melting point of PLGA. The melting enthalpy (Delta Hf) was observed at 103.1410J/g and the area of peak was 825.128 mJ, with a peak height of 2.8229 mW (6). The DSC thermogram obtained for Lycopene, PLGA and physical mixture of drug polymers has been compared. The DSC thermograms show a broad endotherm at 175.60^{0}C for Lycopene and PLGA at 295^{0}C. In the physical mixture the endothermic of Lycopene and PLGA, were in their respective position. This implies the nonreactive nature of PLGA and other excipients with Lycopene, Figure No 3. Presence of drug peak in DSC thermogram of the prepared physical mixture indicates compatibility of drug with polymer (48, 51,52).

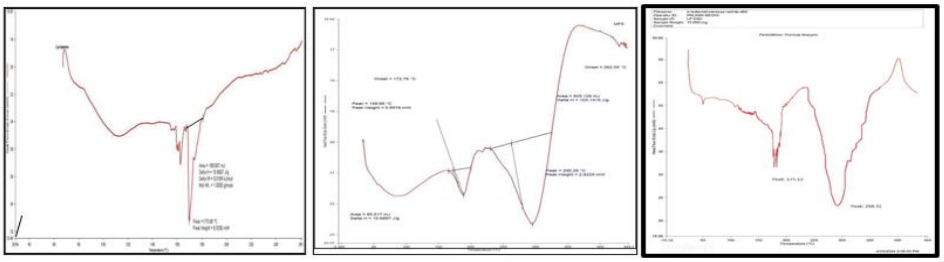

Figure 3: A. DSC thermogram of Lycopene, B is The DSC thermogram of PLGA and C is the DSC thermogram of of physical mixture. The presence of both endothermic peaks I.e Lyvopene and PLGA in the DSC of the physical mixture indicates excellent drug excipient compatiblity.

6.2 Design Expert

In order to optimize the conditions and observed responses of the obtained 17 formulations in this study, the Box-Behnken design (BBD) was employed using Design-Expert Software (version 10.0.3). This statistical software is renowned for its capabilities in designing experiments and analyzing the resultant data, particularly in the context of response surface methodology (RSM). The upper and lower- level limits for each independent variable were fitted. The selected independent variable including the quantity of sodium alginate, tween 80 and stirring speed of magnetic stirrer significantly influence observed responses for particle size, PDI, zeta potential and drug entrapment efficiency. The design- expert software produced polynomial equations that described the specific main effect and interaction effect of independent factors on each dependent factors. The result of the following is shown in the Table No 2.

Table No 2: Selected factors and observed responses from design expert.

Std	Run	Factor 1 A: Sodium Alginate (mg)	Factor 2 B: Tween 80 (ml)	Factor 3 C: Stirring Speed (rpm)	Response 1 Particle Size (nm)	Response 2 Zeta Potential (mV)	Response 3 Drug Entrapment Efficiency (%)
8	1	10	0.55	6000	229.12	-24.8	67.14
13	2	5.5	0.55	4000	120.89	-22.6	79.4
7	3	1	0.55	6000	147.35	-23.6	68.59
16	4	5.5	0.55	4000	110.29	-20.8	79.56
2	5	10	0.1	4000	109.56	-14.2	71.69
4	6	10	1	4000	123.53	-20.3	69.20
3	7	1	1	4000	94.43	-16.8	76.12
14	8	5.5	0.55	4000	96.34	-17.6	81.56
6	9	10	0.55	2000	75.31	-11.6	71.49
15	10	5.5	0.55	4000	121.8	-18.9	79.61
11	11	5.5	0.1	6000	133.6	-22.9	78.46
5	12	1	0.55	2000	65.91	-12.9	76.46
17	13	5.5	0.55	4000	116.7	-16.9	76.16
9	14	5.5	0.1	2000	87.21	-12.9	77.53
12	15	5.5	1	6000	296.43	-25.4	58.23
1	16	1	0.1	4000	90.26	-15.5	74.89
10	17	5.5	1	2000	52.95	-10.6	75.20

The suggested particle size of the nano formulations was found to be falling within the range of 52.95 to 296.43 nm. Moreover, the zeta potential was found to be falling in the range of -10.6 to -25.4 mV along with drug entrapment efficiency in range of 58.23% - 81.56% respectively.

6.2.1 Effect on Particle Size

The following equation explains the influence of different factors on particle size response which was generated as

Particle Size = $+113.20+17.45*A+ 18.34*B+65.64*C+2.45*AB+18.09*AC+49.27*BC-10.94*A^2 +2.18*B^2+27.16*C^2$……..eq1

The determination of the 'p-value/ Prob > F' was found to be 0.0006 which is less than 0.0500 indicating the **Quadratic model to be significant.** In this case, A, B, C, BC and C^2 are significant model terms. Values greater than 0.1000 indicate the model terms are not significant. The lack of fit value is found to be 0.0515 being greater than 0.0500 indicating it to be not significant, which implies that the model was adequate for prediction with the range of the experimental values. From the data it is seen that the amount of sodium alginate and tween 80 were the main factors that influenced the particle size.

Lower amount of sodium alginate and higher concentration of tween 80 decreases the particle size, whereas higher the concentration of sodium alginate higher the particle size. Moreover, the amount of tween 80 and sodium alginate have maintained the medial level with particle size. Thus, the levels of tween 80 and sodium alginate were found to be favorable for the formulation.

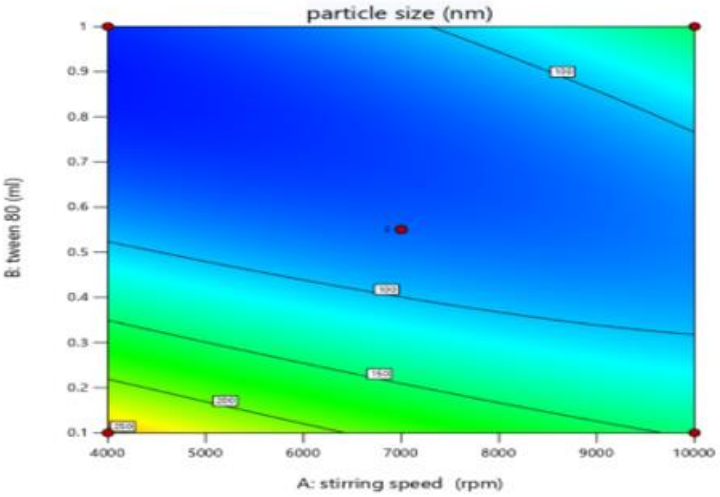

Figure No 4 : Contour graph of particle size

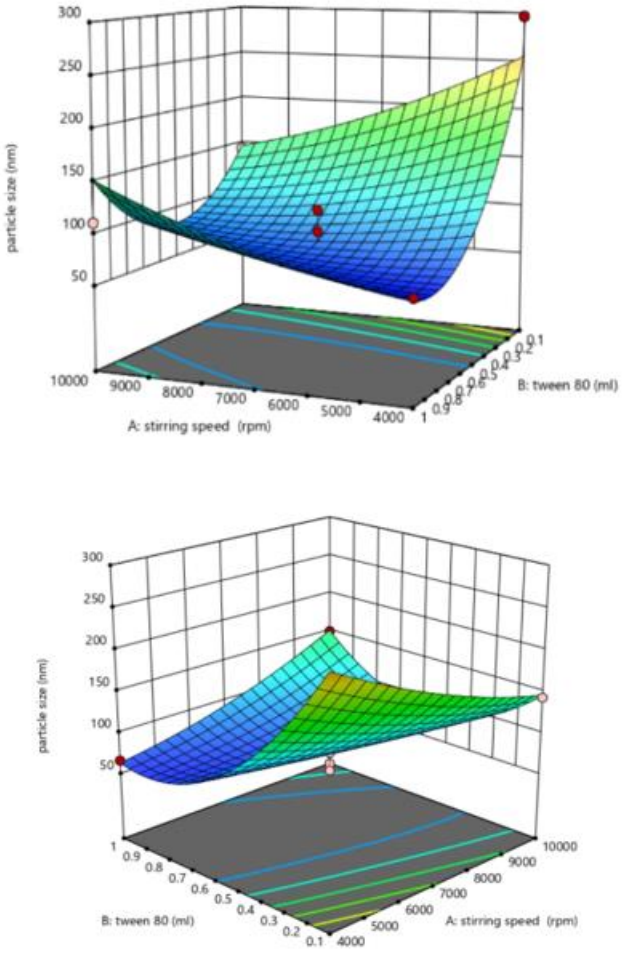

Figure No.5: 3D-Analysis graph of Particle Size

6.2.2 Effect on Zeta Potential

The following equation explains the influence of different factors on particle size response which was generated as
Zeta Potential= -18.36-1.50*A+4.40*B+1.25*C…….eq 2

The determination of the 'p-value/ Prob > F' was found to be 0.0132 which is less than 0.0500 indicating the **Linear model to be significant.** In this case, B, are significant model terms. Values greater than 0.1000 indicate the model terms are not significant. The lack of fit value is found to be 0.9200 being greater than 0.0500 indicating it to be not significant, which implies that the model was adequate for prediction with the range of the experimental values. From the data it is seen that the amount of sodium alginate and tween 80 were the main factors that influenced the zeta potential. Lower amount of sodium alginate and higher concentration of tween 80 decreases the zeta potential, whereas higher the concentration of sodium alginate increases the zeta potential. Moreover, the quantity for Tween 80 alonside Sodium alginate have maintained the medial level with zeta potential. Thus, the levels of aforesaid parameters were found to be favorable for the formulation.

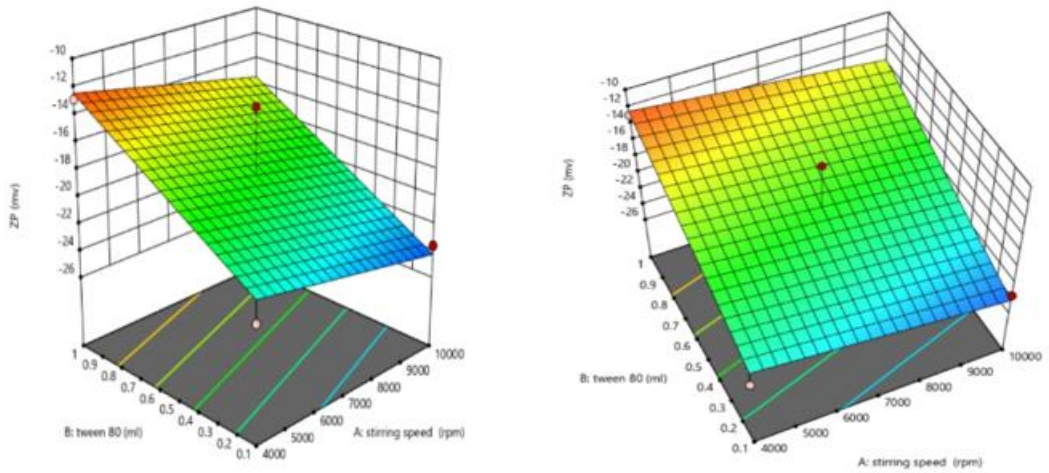

Figure No. 6: A. Contour graph for zeta potential, B&C 3-D-Analysis graph of Zeta Potential.

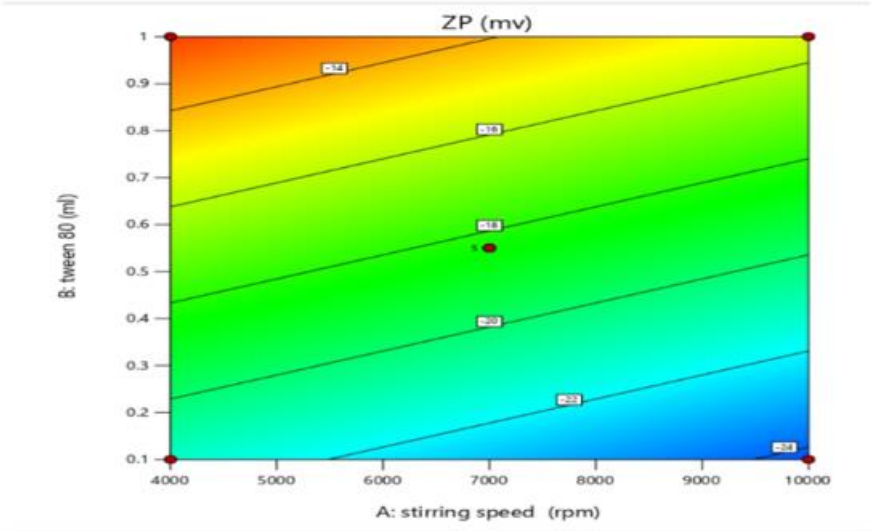

Contour graph of Zeta Potential

Effect on Drug Entrapment Efficiency (EE)

The equation illustrated below explains the impact of different factors on particle size response which was generated as ,
DE= =74.14-0.1500*A-0.6113*B+0.7713*C+0.3725*AB-1.96*AC+1.50*BC-0.8760*A^2-0.6585*B^2-3.83*C^2

The determination of the 'p-value/ Prob > F' was found to be 0.0347 which is less than 0.0500 indicating the **Quadratic**

model to be significant. In this case, AC and C^2 are significant model terms. Values greater than 0.1000 indicate the model terms are not significant. The lack of fit value is found to be 0.9200 being greater than 0.1873 indicating it to be not significant, which implies that the model was adequate for prediction with the range of the experimental values. From the data it is seen that the quantity of Tween 80 and Sodium alginate were the main factors that influenced the drug entrapment efficiency. Fig no. shows higher quantity of Sodium Alginate used (around 4-6 mg) and moderate amounts of Tween 80 (around 0.3-0.5 ml) result in higher entrapment efficiency (around 80%). As the amounts of Tween 80 and Sodium Alginate move away from these optimal values, the entrapment efficiencyof Lycpene decreases, reaching as low as 68% in the top-right and bottom-left corners. Moreover, the amount of tween 80 and Sodium Alginate have maintained the medial level with drug entrapment. Thus, the explained quantity Sodium alginate and Tween 80, were found to be favorable for the formulation.

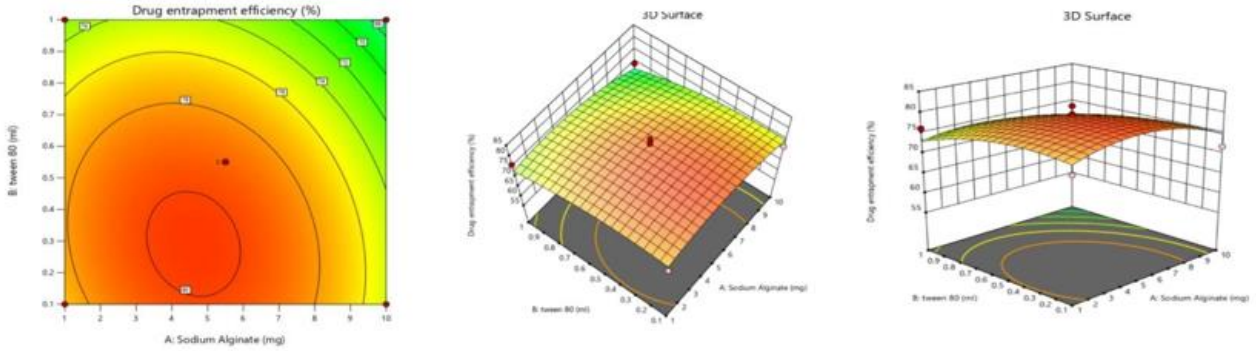

Figure No 7: A. Contour graph for drug entrapment efficacy, B&C represent the the 3-D analysis of drug entrapment efficacy.

Optimized Solution

The optimized predicted solution was observed by the design expert after analysis and found to be significant given in Table No. 6.3

Table No. 3 Optimized formulation solution

SOLUTION							
Number	**Sodium Alginate**	**Tween 80**	**Stirring Speed**	**Particle Size**	**Zeta Potential**	**Drug Entrapment Efficiency**	**Desirability**
F1	7.829	0.168	3296.426	128.389	-15.324	77.537	1.000

6.2.5 Post-analysis solution, confirmation and characterization of Lycopene- loaded PLGA nanoparticles.

The post- analysis of the optimized solution was observed after preparing the optimized formulation and calculating the mean value of the responses, the post point prediction and confirmation are given below in **Table no. 4**

Particle size and zeta potential (ζ) :

The particle size of the final optimized formulation was determined by using Litisizer (Antor Paar). The particle size of the final optimized formulation was found to be in the range of predicted interval. Indicating that the prepared formulations was optimized.

The particle size and zeta potential of the optimized formulation was found to be 157.40 nm and -17.1mV respectively. Booth the values indicate an excellent colloidal stability of the ptimized formulation. Moreover after conjugation of the formulation with the monoclonal antibody Cetuximab, the particle size was found to be 183.8 nm and zeta potential was -15.3mV, indicative of a good colloidal stability after surface modification with Cetuximab, Figure 8 (A,B).

Table No. 4: Confirmation and characterization of optimized Lycopene- loaded PLGA Nanoparticles.

Responses	**Predicted mean**	**Standard Deviation (SD)**	**Observed mean**
Particle size	118.648	36.5685	157.40 nm
Zeta potential	-18.1353	2.11526	-17. 7 mV

Drug Entrapment	79.258	3.28152	76.41%

Percentage yield of PLGA nanoparticles
The percentage yield of the optimized PLGA nanoparticles was calculated and it was found to be around 73.66%.

6.4 Drug Loading and Entrapment Efficiency Determination
The drug loading and drug entrapment efficiency of the optimized formulation was being analysed spectrophotometrically by UV-Vis spectroscopy (Shimadzu, 1800). The drug loading was found to be 37.2% and drug entrapment was found to be 76.4% respectively.

6.5 Morphological analysis using High-Resolution Transmission Electron Microscopy (HRTEM)
The optimized Cetuximab conjugated formulation was scanned under High-Resolution Transmission Electron Microscopy. The nanoparticles were observed under 500x to 15000x magnification. The nanoparticles were found to be spherical and had smooth surfaces as seen in the results, but showed an aggregated appearance and orientation . The size of the nanoparticles of 50 to 100 nm. . The images suggest that drug was dwas uniformly distributed throughout the matrix of the PLGA nanaoparticles. The size of the nanoparticles were on the higher side as observed in dynamic light scattering studies (DLS), in contrast to HR TEM, because of the swelling effect of the polymer, as DLS studies were carried out by dispersing the nanoparticles in a solvent and resulted in hydrated surface layers of the nanoparticles, hence an increase in particle size in contrast to HR TEM was recorded under dry state obtained after freeze drying. Moreover, we can clearly see in Figure No 8 (D,E) that the HR TEM images that there is aggregation and surface adhesion of the PLGA nanoparticles which is due to the coating of Alginate on the surface of nanoparticles, which leads to adhesion.

Nuclear Magnetic Resonance Spectroscopy for Cetuximab- Conjugated Nanoparticles
NMR (Nuclear Magnetic Resonance) spectroscopy data for Cetuximab-conjugated PLGA nanoparticles is shown in figure no.6.29 respectively. NMR was determined using Ascend 500, Bruker. Interpreting the 1^11H NMR spectrum for cetuximab-conjugated PLGA nanoparticles involves analysing the chemical shifts, peak intensities, and splitting patterns to identify the different proton environments in the sample. α-Protons to amides (N-CH) usually appear between 2-4 ppm. Resonances from protons directly attached to the carbon bonded to nitrogen in an amide tend to resonate in the 2.0-3.0 ppm region of an NMR spectra. The NH protons of primary and secondary amides resonate in the 5.5-8.5 ppm regions. There are peaks in this region (2-3ppm), which correspond to protons on carbons adjacent to the amide nitrogen ($N\text{-}CH_2$ or N-CH). Protons attached to the aromatic ring in phenols show up near the aromatic region of an NMR spectrum (7-8 ppm). These peaks will have splitting typical for aromatic protons. The region between 2-2.2 ppm indicated the presence of ester bonds of PLGA. The spectrum indicates successful conjugation of cetuximab to PLGA nanoparticles. The presence of peaks characteristic of both PLGA (ester protons) and cetuximab (aromatic and specific amino acid side chains) suggests that the conjugation process was successful (8, 9).

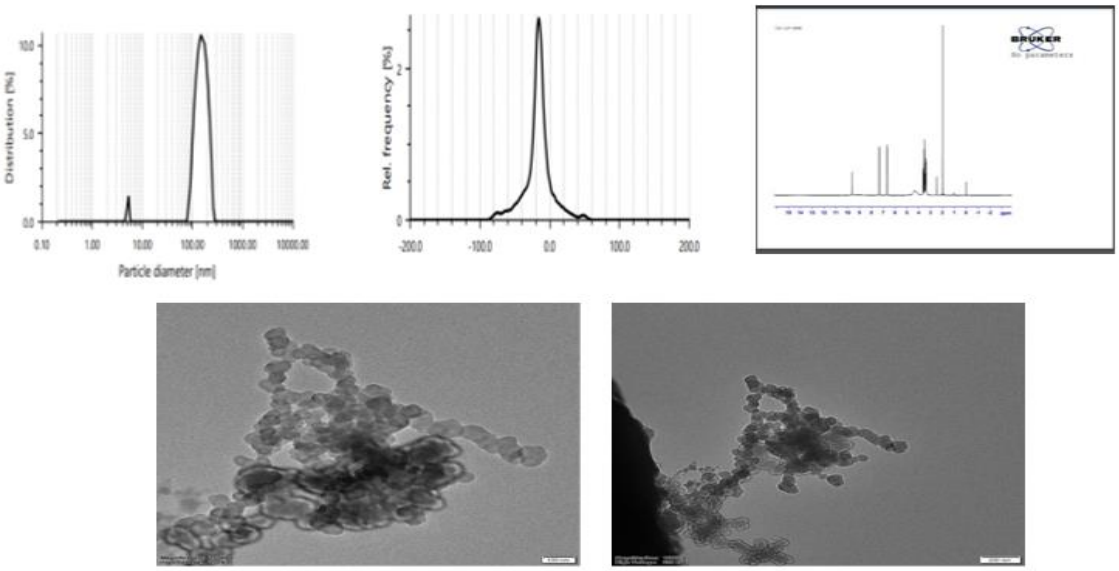

Figure 8: A. Particle size of nanoparticles, B is zeta potential of nanoparticles, C is the NMR spectrum of Cetuximab conjugated PLGA nanoparticles. Dand E are High resolution TEM images of Cetuximab conjugated nanoparticles.

Fourier Transform Infrared Spectroscopy (FTIR) for Cetuximab- Conjugated Nanoparticles.

The appearance of an N-H stretch peak at 3262.60 cm^{-1} in the conjugated sample indicates the occurence of amine groups from Cetuximab, which are absent in the blank form PLGAformulation**.** The shift from 1628.00 cm^{-1} to 1649.32 cm^{-1} suggests an interaction between the PLGA and Cetuximab, possibly due to involvement of new bonds involving the carbonyl group. The shift from 1100.91 cm^{-1} to 1074.71 cm^{-1} suggests a change in the local environment of the ether bonds in PLGA, likely due to the presence of cetuximab. By carefully analysing these shifts and new peaks, you can confirm the conjugation of cetuximab to PLGA nanoparticles (10, 11).

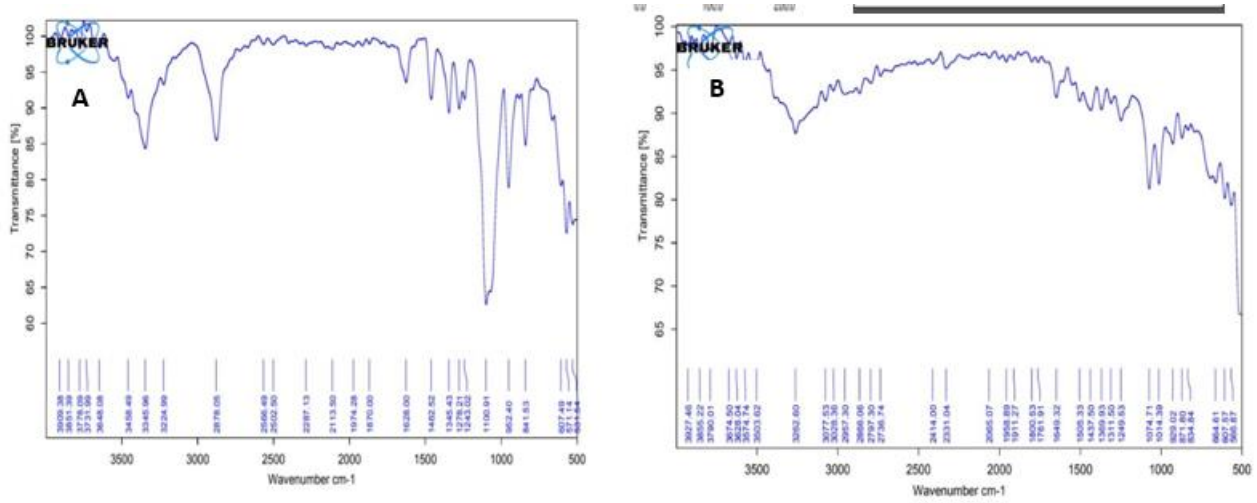

Figure 9 : IR spectrum of A.Balank PLGA nanoparticles, B. Cetuximab conjugated nanoparticles, a justification of conjugation of Cetuximab to the PLGA surface.

6.8 Execution of In- Vitro Drug Release study

The *in vitro* release behaviour of the formulation that was optimized after loading with Lycopene and conjugated with Cetuximab was investigated using dialysis membrane method in phosphate buffer 7.4 and 6.8 for a period of 12hrs. The in -vitro release of drug from the optimized formulation was determined from the absorbance (Shimadzu-1800). From the in vitro drug release, the drug release in 12hrs was found to be 74.1%.

6.8.1 In- Vitro drug release kinetics study

In order to understand the mechanism as well as the kinetics of drug release from the prepared optimized formulation, various kinetic models such as zero order, first order, Higuchi, Korsmeyer Peppas and Hixon Crowell models were plotted.

Table no.5: Kinetic modelling of in vitro drug release data

Buffers	**Zero Order release**	**First Order release**	**Higuchi**	**Korsmeyer- Peppas**			**Hixon Crowell**
	R^2	**R^2**	**R^2**	**R^2**	**k**	**n**	**R^2**
PB 7.4	0.748	0.823	0.8507	0.973	0.3529	0.1302	0.42
PB 6.8	0.871	0.851	0.732	0.947	0.4554	0.6439	0.45

Looking at the **R^2** values, the Korsmeyer-Peppas model is the best fitted model for both the media since R^2 was closest to 1. Therefore, the drug release mechanism of the optimized nanoparticles is based on the Korsmeyer-Peppas kinetics which is known to describe drug release from polymeric systems. Also, the value of **'n'** and **'k'** from the Korsmeyer-Peppas equation: ln(M∞Mt)=ln(k)+nln(t) was calculated. For phosphate buffer 6.8, the value of **n** and **k** were 0.6439 and 0.4554 respectively. For PBS 7.4, the value of **n** and k were 0.1302 and 0.3567. **k** is the release rate constant in the Korsmeyer-Peppas model, which quantifies the rate at which drug molecules are released from the delivery system over time. Here, the value of **k** is higher in phosphate buffer 6.8 indicating faster release rate in acidic medium then in PBS 7.4**. n** is the release exponent in the Korsmeyer-Peppas model, which characterizes the release mechanism and the kinetics of drug release. The value of **n** for phosphate buffer 6.8 is between 0.43 and 0.85 which shows Anomalous (non-Fickian) transport,

indicating a combination of diffusion and polymer relaxation or erosion. The value of n for PBS 7.4 is ≤0.43 which shows Fickian diffusion, where drug release is primarily controlled by molecular diffusion through the polymer matrix (12-14).

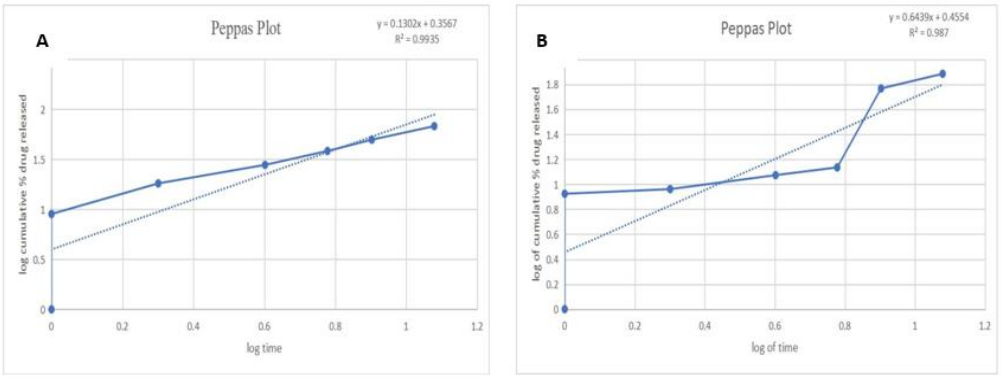

Figure 10: A is invitro release kinetic modelling in phosphate buffer pH 7.4 and B. is in vitro release kinetic study in Phosphate buffer pH 6.8 and the R values indicate that both follow korsmeyer Peppas kinetics.

Haemolysis study and Assay:
Haemolysis percentage of 3.25% for PLGA nanoparticles signifies that these nanoparticles cause minimal damage to RBCs under the specified experimental conditions. This interpretation supports the potential biocompatibility of PLGA nanoparticles for various biomedical applications, indicating their safety profile with respect to blood cell interactions (15,16).

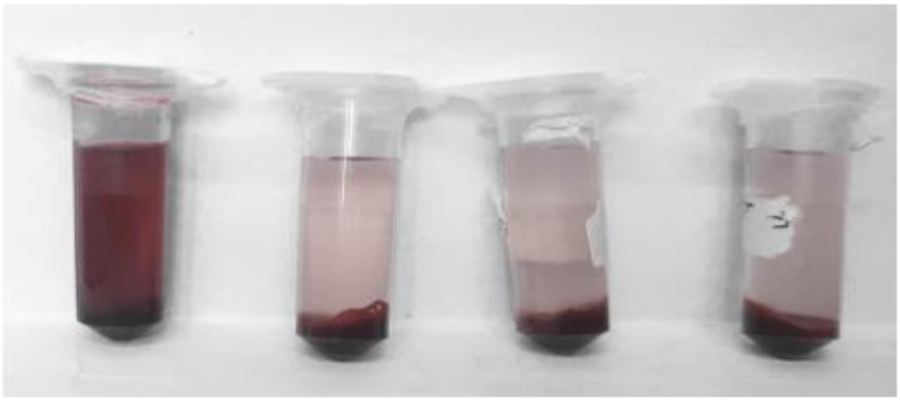

Figure 11: Haemolysis Study carried out in different media

1. **A-**Positive Control (Tap Water)
2. **B-**Negative Control (0.9% NaCl)
3. **C**-Blank PLGA (Blank PLGA formulation diluted with PBS)
4. **D**-Cet-PLGA (Cetuximab-conjugated PLGA nanoparticles dissolved in PBS)

Calculation of Haemolysis Percentage:
The Hemolysis percentage was calculated using the Drabkins reagent and it was found to be 3.25% indicating that the Cetuximab conjugated PLGA nanoparticles cause no harm to the RBC's.

Bradford Protein Assay for quantification of Cetuximab:
Bradford Protein Assay was performed for the optimized cetuximab conjugated PLGA nanoparticles. The standard curve is given in **Fig No**.12

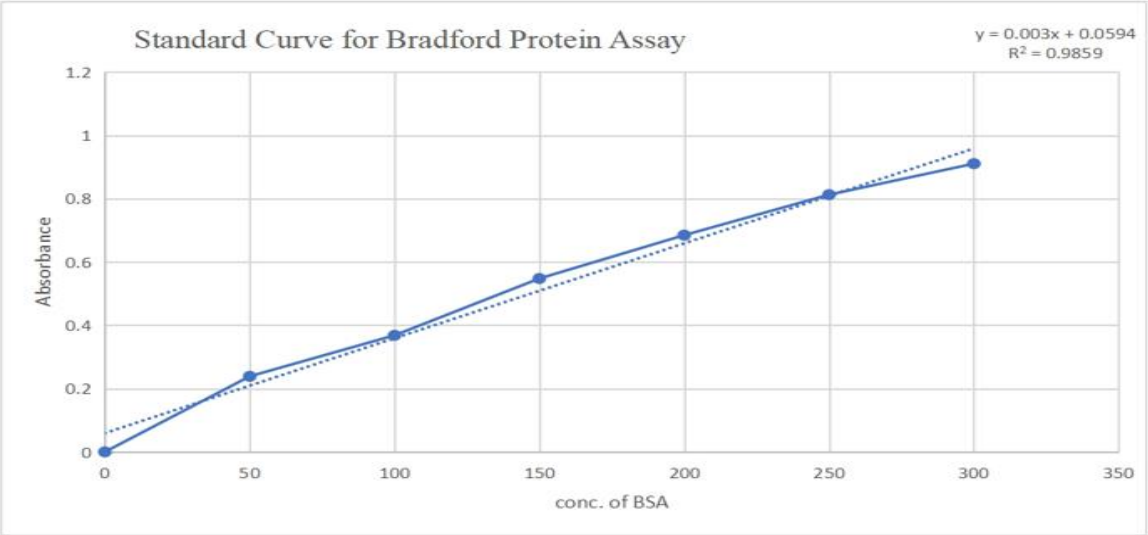

Figure No.12: Standard Curve for Bradford Protein Assay

Table No.6: Protein Concentration for Cetuximab Conjugated PLGA nanoparticles

Sample ID	**Absorbance (595nm)**	**Protein Concentration (µg/mL)**
Cet-PLGA 1	0.89	279.06
Cet-PLGA 2	0.72	220.2
Cet- PLGA 3	0.75	230.2

The Bradford assay measures protein concentration based on the absorbance of Coomassie Brilliant Blue dye bound to proteins. Higher absorbance values correlate with higher protein concentrations. The consistent protein concentration values indicate that cetuximab was successfully conjugated to the PLGA nanoparticles. The average protein concentration across the three samples was calculated to be 243.1± 0.05 µg/ml. This finding supports that the Bradford protein assay confirms the successful conjugation of cetuximab to PLGA nanoparticles (17,41,42).

MTT Assay on PANC-1 Cells:

We did a comparative evaluation of the cytotoxic potential of Lycopene (LY), Lycopene loaded Alginate -PLGA Nanoparticles (PL-LY) and Cetuximab conjugated PLGA nanoparticle (Cet-LY-PLGA) on PANC -1 cells. It was found that the cytotoxicity of Cetuximab conjugated nanoparticles was highly increased in comaprison to LY and PL-LY. Cytotoxicity values (IC_{50}) are specified in the Table No. 7.

We propose that this is due to the fact that EGF, antibodies such as cetuximab selectively bind to the overexpressed EGFR on the surface of cancer cells making them a perfect ligant for active targetting. The incresed cytotoxicity of Cet-LY-PLGA nanoparticles is Internalisation through endocytic pathways, mainly clathrin-mediated endocytosis, is the result of receptor-mediated endocytosis, which is triggered by this binding and causes EGFR on the cell membrane to activate and aggregate nanoparticles inside the PANC-1 cells (42,44).

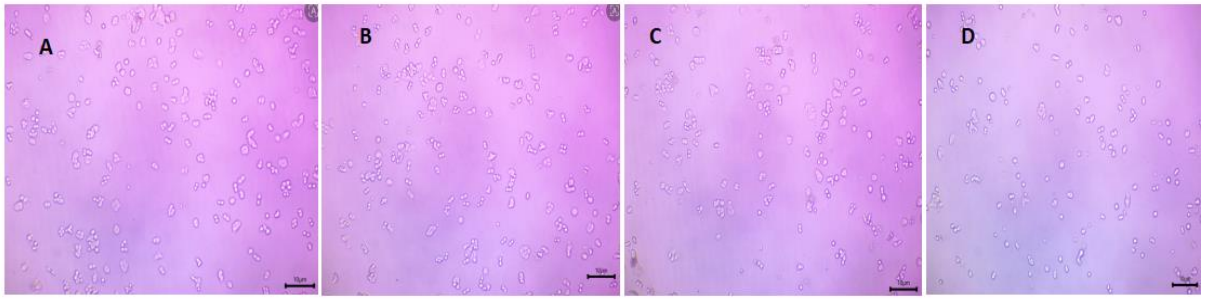

Figure 13: ***A represents control group, B represents Lycopene (LY) treated PANC-1 cells, C represents Lycopene encapsulated Alginate-PLGA nanoparticles (PL-LY) treated group and D represents Cetuximab conjugateed Alginate PLGA nanoparticles (Cet-LY-PLGA) treated group, p value was < 0.05, Kruskal-wallis test was performed.***

CODE	IC $_{50}$ VALUE
LY	350 ± 0.03 µM
PL-LY	135 ± 0.05 µM
Cet-LY-PLGA	55 ± 0.06 µM

Table 7: IC 50 values of different formulations.

4. CONCLUSION:

Research into more potent and specialised treatments is still ongoing because pancreatic cancer is still one of the most fatal types of cancer worldwide. Drug delivery methods based on nanoparticles have demonstrated significant promise in improving the effectiveness and specificity of cancer therapies. This study aims to cure pancreatic cancer by creating cetuximab-conjugated Alginate-poly(lactic-co-glycolic acid) (PLGA) nanoparticles loaded with lycopene. Although lycopene, a strong antioxidant found in tomatoes, has shown strong anti-cancer effects, its poor solubility and stability limit its therapeutic use. Lycopene is encapsulated in matrix of Alginate and PLGA, a biocompatible and biodegradable polymer mix, which increases its solubility , encapsulation efficacy, durability and guarantees a regulated release. Cetuximab is an inhibitor of the epidermal growth factor receptor (EGFR).is attached to the nanoparticles' surface to target pancreatic cancer cells that overexpress EGFR, improving the treatment's specificity.Preformulation research was essential to the creation of the PLGA nanoparticles loaded with lycopene. In this context, a number of tests were carried out, including the analysis of the thermal characteristics of Lycopene, PLGA, and the nanoparticle formulation using Differential Scanning Calorimetry (DSC). According to the DSC thermograms, Lycopene was amorphously distributed throughout the PLGA matrix, indicating that the medicine and polymer were compatible and that encapsulation had been successful. Utilising Fourier Transform Infrared Spectroscopy (FTIR), the chemical stability and integrity of the Lycopene within the nanoparticles were verified. Lycopene and MPLGA's distinctive peaks in the FTIR spectra demonstrated that the encapsulation technique had no effect on the chemical structure of lycopene.To attain the required particle size, zeta potential, and drug encapsulation effectiveness, a number of factors were methodically adjusted, including the formulation's stirring speed (rm) and the content of sodium alginate and surfactant (tween 80).

The optimised nanoparticles demonstrated a negative zeta potential, a good drug loading and encapsulation capacity, and an average particle size of roughly 154 nm.

Over time, therapeutic amounts of lycopene are maintained by the nanoparticles' prolonged release pattern.The Bradford protein assay and haemolysis studies were used to verify the nanoparticles' biocompatibility and efficient targeting capabi lities.These results imply that the efficacy and specificity oftreatment for pancreatic cancer may be enhanced by this nano particle formulation.For possible clinical usage, the formulation's quality and safety are also essential.A number of variables, including the formulation's stirring speed (rpm) and the quantity of sodium alginate and surfactant (Tween 80), were methodically adjusted to produce the required zeta potential, particle size, and drug encapsulation effectiveness. Hence this is a very a promising and neoteric drug delivery strategy to target pancreatic cancer.

Acknowledgements:
The authors thank Sophisticated Analytical Instrumentation Centre (SAIC), Institute of Advanced Study in Science and Technology (IASST), Guwahati (under the Department of Science & Technology, Government of India) for nanoparticle sample analysis"
The author of this paper would sincerely like to thank the Department of science and Technology, government of India for fundig this work Under the Women Scientist A scheme, DST/WOS-A/LS-298/2019.
The author group also would like to extend thanks to DBT (NER), AICTE (RPS), DRDO, DST for providing the support.

Conflict of interest statement: *The authors declare that there is no conflict of Interest in this research work.*
Data availability statement: *All the experimental data associated with this study is available on request.*

REFRANCES:

1. Surveillance, Epidemiology, and End Results Program, Seer Cancer Statistics Review, 1973–1994: Tables and Graphs,National Cancer Institute, Bethesda, MD, 1997, Google Scholar.
2. Yeo, C.J. · Cameron, J.L.Pancreatic cancer Curr. Probl. Surg. 1999; 36:59-152Crossref PubMed, Google Scholar.
3. 4.Khachik, F. · Askin, F.B. · Lai, K., Distribution, bioavailability, and metabolism of carotenoids in humans,Technimin Publishing, Lancaster, PA, Bidlack, W.R. · Omaye, S.T. · Meskin, M.S. ... (Editors),in:

Phytochemicals: A New Paradigm. 1998, Google Scholar.
4. 5.Zhang, L.X. · Cooney, R.V. · Bertram, J.S., Carotenoids enhance gap junctional communication and inhibit lipid peroxidation in C3H/10T1/2 cells: relationship to their cancer chemopreventive action, Carcinogenesis. 1991; 12:2109-2114, Crossref, Scopus (492), PubMed Google Scholar
5. 6.Cooper, D.A. · Eldridge, A.L. · Peters, J.C., Dietary carotenoids and certain cancers, heart disease, and age-related macular degeneration: a review of recent researchNutr. Rev. 1999; 57:201-214,Crossref, Scopus (132) PubMed, Google Scholar
6. 7.Palozza, P. · Serini, S. · Torsello, A. ...β-Carotene regulates NF-κB DNA binding activity by a redox mechanism in human leukemia and colon adenocarcinoma cellsJ. Nutr. 2003; 133:381-388, Full Text,Full Text (PDF),Scopus (124),PubMedGoogle Scholar
7. 8.Herber, D. · Lu, Q.Y. Overview of mechanism of action of lycopene Exp. Biol. Med. 2002; 227:920-923,Crossref,Scopus (426) Google Scholar
8. 9.Nishino, H. · Tokuda, H. · Murakoshi, M. ...Cancer prevention by natural carotenoids, Biofactors. 2000; 13:89-94.
9. 10.Singh M, Pal P, Dutta RS, Marbaniang D, Ray S, Mazumder B. Nanodiamond Mediated Molecular Targeting in Pancreatic Ductal Adenocarcinoma: Disrupting the Tumor-stromal Cross-talk, Next Hope on the Horizon? Curr Cancer Drug Targets. 2023;23(8):620-633. doi: 10.2174/1568009623666230227120837. PMID: 36843367.
10. 11.White DA, Ornsrud R, Davies SJ. Determination of carotenoid and vitamin a concentrations in everted salmonid intestine following exposure to solutions of carotenoid in vitro. Comp Biochem Physiol A Mol Integr Physiol. 2003;136(3):683–92. doi: 10.1016/s1095-6433(03)00222-8. [DOI] [PubMed] [Google Scholar]
11. 12.Chen YJ, Inbaraj BS, Pu YS, Chen BH. Development of lycopene micelle and lycopene chylomicron and a comparison of bioavailability. Nanotechnology. 2014;25(15):155102. doi: 10.1088/0957-4484/25/15/155102. [DOI] [PubMed] [Google Scholar]
12. 13.Gomes GVdL, Borrin TR, Cardoso LP, Souto E, Pinho SCd. Characterization and shelf life of ²-carotene loaded solid lipid microparticles produced with stearic acid and sunflower oil. Braz Arch Biol Techn. 2013;56(4):663–71. [Google Scholar]
13. 14.Hejri A, Khosravi A, Gharanjig K, Hejazi M. Optimisation of the formulation of beta-carotene loaded nanostructured lipid carriers prepared by solvent diffusion method. Food Chem. 2013;141(1):117–23. doi: 10.1016/j.foodchem.2013.02.080. [DOI] [PubMed] [Google Scholar]
14. 15.Riangjanapatee P, Muller RH, Keck CM, Okonogi S. Development of lycopene-loaded nanostructured lipid carriers: Effect of rice oil and cholesterol. Pharmazie. 2013;68(9):723–31. [PubMed] [Google Scholar]
15. 16.Eskandani M, Barar J, Dolatabadi JE, Hamishehkar H, Nazemiyeh H. Formulation, characterization, and geno/cytotoxicity studies of galbanic acid-loaded solid lipid nanoparticles. Pharm Biol. 2015;53(10):1525–38. doi:
16. 10.3109/13880209.2014.991836. [DOI] [PubMed] [Google Scholar]Thi Oanh H, Hac Thi N, Nhan Nguyen T, Anh Dang Thi T, Van Nguyen T, Hoang MH. Co-Encapsulation of Lycopene and Resveratrol in Polymeric Nanoparticles: Morphology and Lycopene Stability. J Nanosci Nanotechnol. 2021 May 1;21(5):3156-3164. doi: 10.1166/jnn.2021.19146. PMID: 33653491.
17. Ardawi MSM, Badawoud MH, Hassan SM, Ardawi AMS, Rouzi AA, Qari MH, Mousa SA. Lycopene nanoparticles promotes osteoblastogenesis and inhibits adipogenesis of rat bone marrow mesenchymal stem cells. Eur Rev Med Pharmacol Sci. 2021 Nov;25(22):6894-6907. doi: 10.26355/eurrev_202111_27238. PMID: 34859851.
18. Goswami A et al., Lycopene loaded polymeric nanoparticles for prostate cancer treatment: Formulation, optimization using Box-behnken design and cytotoxicity studies ,V 67, DO - 10.1016/j.jddst.2021.102930 JO ,Journal of Drug Delivery Science and Technology
19. Carvalho GC, Marena GD, Leonardi GR, Sábio RM, Corrêa I, Chorilli M, Bauab TM. Lycopene, Mesoporous Silica Nanoparticles and Their Association: A Possible Alternative against Vulvovaginal Candidiasis? Molecules. 2022 Dec 5;27(23):8558. doi: 10.3390/molecules27238558. PMID: 36500650; PMCID: PMC9738730.
20. Mennati A, Rostamizadeh K, Manjili HK, Fathi M, Danafar H. Co-delivery of siRNA and lycopene encapsulated hybrid lipid nanoparticles for dual silencing of insulin-like growth factor 1 receptor in MCF-7 breast cancer cell line. Int J Biol Macromol. 2022 Mar 1;200:335-349. doi: 10.1016/j.ijbiomac.2021.12.197. Epub 2022 Jan 6. PMID: 34999039.
21. T1 - Preparation of enzymatically cross-linked α-lactalbumin nanoparticles and their application for encapsulating lycopene, 429, 10.1016/j.foodchem.2023.136394,JO - Food Chemistry.
22. 23..Seufferlein T, Bachet J, Van Cutsem E, Rougier P; ESMO Guidelines Working Group. Pancreatic adenocarcinoma: ESMO–ESDO clinical practice guidelines for diagnosis, treatment and follow-up. Ann Oncol. 2012;23(suppl_7):vii33–vii40. [DOI] [PubMed] [Google Scholar]
23. 24.Oliveira-Cunha M, Newman WG, Siriwardena AK. Epidermal growth factor receptor in pancreatic cancer. Cancers. 2011;3(2):1513–1526. doi: 10.3390/cancers3021513 [DOI] [PMC free article] [PubMed]

[Google Scholar]
24. 25.Vaccaro V, Melisi D, Bria E, et al. Emerging pathways and future targets for the molecular therapy of pancreatic cancer. Expert Opin Ther Targets. 2011;15(10):1183–1196. doi: 10.1517/14728222.2011.607438 [DOI] [PubMed] [Google Scholar]
25. 26.Beraldo-Araújo VL, Flávia Siqueira Vicente A, van Vliet Lima M, Umerska A, Souto EB, Tajber L, Oliveira-Nascimento L. Levofloxacin in nanostructured lipid carriers: Preformulation and critical process parameters for a highly incorporated formulation. Int J Pharm. 2022 Oct 15;626:122193. doi: 10.1016/j.ijpharm.2022.122193. Epub 2022 Sep 13. PMID: 36108993.
26. 27.Astete CE, Sabliov CM. Synthesis and characterization of PLGA nanoparticles. J Biomater Sci Polym Ed. 2006;17(3):247-89. doi: 10.1163/156856206775997322. PMID: 16689015.
27. Amir Kalvanagh P, Ebtekara M, Kokhaei P, Soleimanjahi H. Preparation and Characterization of PLGA Nanoparticles Containing Plasmid DNA Encoding Human IFN-lambda-1/IL-29. Iran J Pharm Res. 2019 Winter;18(1):156-167. PMID: 31089352; PMCID: PMC6487415.
28. 29.Bultelle M, Casas A, Kitney R. Construction of a Calibration Curve for Lycopene on a Liquid-Handling Platform─Wider Lessons for the Development of Automated Dilution Protocols. ACS Synth Biol. 2024 Aug 16;13(8):2357-2375. doi: 10.1021/acssynbio.4c00031. Epub 2024 Aug 3. PMID: 39096303; PMCID: PMC11334188.
29. 30.Rashid MA, Muneer S, Wang T, Alhamhoom Y, Rintoul L, Izake EL, Islam N. Puerarin dry powder inhaler formulations for pulmonary delivery: Development and characterization. PLoS One. 2021 Apr 13;16(4):e0249683. doi: 10.1371/journal.pone.0249683. PMID: 33848310; PMCID: PMC8043385.
30. 31.Ledeți I, Romanescu M, Cîrcioban D, Ledeți A, Vlase G, Vlase T, Suciu O, Murariu M, Olariu S, Matusz P, Buda V, Piciu D. Stability and Compatibility Studies of Levothyroxine Sodium in Solid Binary Systems-Instrumental Screening. Pharmaceutics. 2020 Jan 10;12(1):58. doi: 10.3390/pharmaceutics12010058. PMID: 31936742; PMCID: PMC7022666.
31. Yoshida MI, Gomes EC, Soares CD, Cunha AF, Oliveira MA. Thermal analysis applied to verapamil hydrochloride characterization in pharmaceutical formulations. Molecules. 2010 Apr 8;15(4):2439-52. doi: 10.3390/molecules15042439. PMID: 20428054; PMCID: PMC6257305.
32. McCall RL, Sirianni RW. PLGA nanoparticles formed by single- or double-emulsion with vitamin E-TPGS. J Vis Exp. 2013 Dec 27;(82):51015. doi: 10.3791/51015. PMID: 24429733; PMCID: PMC4106449.
33. 34.Winkler JS, Barai M, Tomassone MS. Dual drug-loaded biodegradable Janus particles for simultaneous co-delivery of hydrophobic and hydrophilic compounds. Exp Biol Med (Maywood). 2019 Oct;244(14):1162-1177. doi: 10.1177/1535370219876554. PMID: 31617755; PMCID: PMC6802157.
34. 35.Ranjan AP, Mukerjee A, Helson L, Vishwanatha JK. Scale up, optimization and stability analysis of Curcumin C3 complex-loaded nanoparticles for cancer therapy. J Nanobiotechnology. 2012 Aug 31;10:38. doi: 10.1186/1477-3155-10-38. PMID: 22937885; PMCID: PMC3497871.
35. 36.Mollaeva MR, Yabbarov N, Sokol M, Chirkina M, Mollaev MD, Zabolotskii A, Seregina I, Bolshov M, Kaplun A, Nikolskaya E. Optimization, Characterization and Pharmacokinetic Study of Meso-Tetraphenylporphyrin Metal Complex-Loaded PLGA Nanoparticles. Int J Mol Sci. 2021 Nov 12;22(22):12261. doi: 10.3390/ijms222212261. PMID: 34830136; PMCID: PMC8618356.
36. 37.Gajra B, Dalwadi C, Patel R. Formulation and optimization of itraconazole polymeric lipid hybrid nanoparticles (Lipomer) using Box Behnken design. Daru. 2015 Jan 21;23(1):3. doi: 10.1186/s40199-014-0087-0. PMID: 25604353; PMCID: PMC4312448.
37. 38.Alshora D, Ibrahim M, Elzayat E, Almeanazel OT, Alanazi F. Defining the process parameters affecting the fabrication of rosuvastatin calcium nanoparticles by planetary ball mill. Int J Nanomedicine. 2019 Jun 27;14:4625-4636. doi: 10.2147/IJN.S207301. PMID: 31303752; PMCID: PMC6603996.
38. 39.Costa MP, Abdu JOC, de Moura MFCS, Silva AC, Zacaron TM, de Paiva MRB, Fabri RL, Pittella F, Perrone ÍT, Tavares GD. Exploring the Potential of PLGA Nanoparticles for Enhancing Pulmonary Drug Delivery. Mol Pharm. 2025 Jul 7;22(7):3542-3562. doi: 10.1021/acs.molpharmaceut.5c00118. Epub 2025 Jun 6. PMID: 40479726; PMCID: PMC12239074.
39. Dutta RS, Elhassan GO, Devi TB, Bhattacharjee B, Singh M, Jana BK, Sahu S, Mazumder B, Sahu RK, Khan J. Enhanced efficacy of β-carotene loaded solid lipid nanoparticles optimized and developed via central composite design on breast cancer cell lines. Heliyon. 2024 Mar 25;10(7):e28457. doi: 10.1016/j.heliyon.2024.e28457. PMID: 38586388; PMCID: PMC10998123.
40. 41.Revilla G, Al Qtaish N, Caruana P, Sainz-Ramos M, Lopez-Mendez T, Rodriguez F, *et al.* Lenvatinib-Loaded Poly(lactic-co-glycolic acid) Nanoparticles with Epidermal Growth Factor Receptor Antibody Conjugation as a Preclinical Approach to Therapeutically Improve Thyroid Cancer with Aggressive Behavior. Biomolecules. 2023 Nov 13;13(11):1647. doi: 10.3390/biom13111647. PMID: 38002329; PMCID: PMC10668968
41. 42.Zumaya ALV, Rimpelová S, Štějdířová M, Ulbrich P, Vilčáková J, Hassouna F. Antibody Conjugated PLGA Nanocarriers and Superparmagnetic Nanoparticles for Targeted Delivery of Oxaliplatin to Cells from Colorectal

Carcinoma. Int J Mol Sci. 2022 Jan 21;23(3):1200. doi: 10.3390/ijms23031200. PMID: 35163122; PMCID: PMC8835878.

42. Vijayalakshmi R, Ambalavanan N, Rajeshkumar S, Mahendra J, Sudhakar U, Parameswari D. Comparative drug release kinetics of Terminalia arjuna mediated SeNPs NanoGel and ZnONPs NanoGel - An in-vitro study. J Oral Biol Craniofac Res. 2025 Jan-Feb;15(1):199-204. doi: 10.1016/j.jobcr.2024.12.011. Epub 2025 Jan 21. PMID: 39906887; PMCID: PMC11791306.
43. 44.Tam AL, Melancon MP, Abdelsalam M, Figueira TA, Dixon K, McWatters A, Zhou M, Huang Q, Mawlawi O, Dunner K Jr, Li C, Gupta S. Imaging Intratumoral Nanoparticle Uptake After Combining Nanoembolization with Various Ablative Therapies in Hepatic VX2 Rabbit Tumors. J Biomed Nanotechnol. 2016 Feb;12(2):296-307. doi: 10.1166/jbn.2016.2174. PMID: 27305763; PMCID: PMC5069970.
44. Dobrovolskaia MA, Clogston JD, Neun BW, Hall JB, Patri AK, McNeil SE. Method for analysis of nanoparticle hemolytic properties in vitro. Nano Lett. 2008 Aug;8(8):2180-7. doi: 10.1021/nl0805615. Epub 2008 Jul 8. PMID: 18605701; PMCID: PMC2613576.
45. Mohanta YK, Nayak D, Mishra AK, Chakrabartty I, Ray MK, Mohanta TK, Tayung K, Rajaganesh R, Vasanthakumaran M, Muthupandian S, Murugan K, Sharma G, Dahms HU, Hwang JS. Green Synthesis of Endolichenic Fungi Functionalized Silver Nanoparticles: The Role in Antimicrobial, Anti-Cancer, and Mosquitocidal Activities. Int J Mol Sci. 2022 Sep 13;23(18):10626. doi: 10.3390/ijms231810626. PMID: 36142546; PMCID: PMC9502095.
46. 47.Tseng SH, Chou MY, Chu IM. Cetuximab-conjugated iron oxide nanoparticles for cancer imaging and therapy. Int J Nanomedicine. 2015 May 20;10:3663-85. doi: 10.2147/IJN.S80134. PMID: 26056447; PMCID: PMC4445874.
47. 48.Balkrishna A, Sharma VK, Das SK, Mishra N, Bisht L, Joshi A, Sharma N. Characterization and Anti-Cancerous Effect of Putranjiva roxburghii Seed Extract Mediated Silver Nanoparticles on Human Colon (HCT-116), Pancreatic (PANC-1) and Breast (MDA-MB 231) Cancer Cell Lines: A Comparative Study. Int J Nanomedicine. 2020 Jan 24;15:573-585. doi: 10.2147/IJN.S230244. PMID: 32158209; PMCID: PMC6986406.
48. 49.Kakwere H, Ingham ES, Tumbale SK, Ferrara KW. Gemcitabine-retinoid prodrug loaded nanoparticles display in vitro antitumor efficacy towards drug-resilient human PANC-1 pancreatic cancer cells. Mater Sci Eng C Mater Biol Appl. 2020 Dec;117:111251. doi: 10.1016/j.msec.2020.111251. Epub 2020 Jul 4. PMID: 32919625; PMCID: PMC7684797.
49. 50.Dobhal K, Verma S, Singh A, Kukreti G. Fabrication and Evaluation of Floating Zidovudine Microbeads for Prolonged Kinetic Release and Bioavailability. Indian Journal of Pharmaceutical Education and Research. 2024 Dec 20;59(1):65-73.
50. Dobhal K, Rautela J, Joshi NC, Jakhmola V. Fabrication of silver nanocomposite of azithromycin and tulsi against in vitro Pseudomonas inhibition. Indian Journal of Pharmacology. 2025 May 1;57(3):120-5.
51. Gill P, Moghadam TT, Ranjbar B. Differential scanning calorimetry techniques: applications in biology and nanoscience. J Biomol Tech. 2010 Dec;21(4):167-93. PMID: 21119929; PMCID: PMC2977967.